THE UNIVERSITY OF MICHIGAN
COLLEGE OF ENGINEERING
Department of Aeronautical and Astronautical Engineering

Quarterly Progress Report

UPPER-ATMOSPHERE STRUCTURE MEASUREMENTS

Submitted for the project by

E. J. Schaefer

UMRI Project 03598

under contract with:

NATIONAL AERONAUTICS AND SPACE ADMINISTRATION
CONTRACT NO. NASw-138
WASHINGTON, D. C.

administered by:

THE UNIVERSITY OF MICHIGAN RESEARCH INSTITUTE ANN ARBOR

April 1960

THE UNIVERSITY OF MICHIGAN PROJECT PERSONNEL
(Both Full-Time and Part-Time)

Brown, John, M. S., Associate Research Engineer
Filsinger, Edward A., Instrument Maker
Glass, David Roger, M.S.E. (Ae.E.), Research Engineer
Gleason, Kermit L., Instrument Maker
Henry, Harold F., Electronic Technician
Jones, Leslie M., B.S., Project Director
Loh, Leslie, M.S., Associate Research Engineer
Mosakewicz, Mary C., Secretary
Nichols, Myron H., Ph.D., Professor of Aeronautical and Astronautical Engineering
Perkins, Ronald J., Assistant in Research
Schaefer, Edward J., M.S., Principal Investigator
Schumacher, Robert, B.S. (E.E.), Assistant in Research
Thornton, Charles, Assistant in Research
Wenk, Norman J., B.S., Research Engineer
Wenzel, Elton A., Research Associate

TABLE OF CONTENTS

LIST OF FIGURES

1. INTRODUCTION

This is the first report on University of Michigan Research Institute Contract NO. NASw-138 describing the development and preparation of instrumentation for measuring the structure of the upper atmosphere which is in progress in the Department of Aeronautical and Astronautical Engineering of The University of Michigan for the National Aeronautical and Space Administration. The program is in continuation of one which was carried out between 27 October 1958 and 1 November 1959 on Contract No. NASw-4. For background material, the reader is referred to the final report on that contract: UMRI Report 2841-1-F.

2. SUMMARY

Progress in the first quarter of the contract is described. A new method of massenfilter operation which will yield total density measurements and provide a backup to the normal method is discussed. The advantages of this type of operation on an occasional basis during flight are presented.

A detailed description of the flight ionizing source and its operation is given. Completed items of the supporting circuitry are described and the attack on those which remain is outlined. The ground station, shown in block form, is composed almost entirely of standard commercial equipment, all of which is on order. All deliveries are expected by April 15.

Finally, the future program is outlined.

3. MASSENFILTER

Tests aimed at a better understanding of the massenfilter and its application to upper-atmosphere structures measurements have continued during the period of the report.

3.1. TOTAL DENSITY MEASUREMENTS

The spectra obtained with the massenfilter using a voltage sweep show a characteristic increase in ion current as zero voltage (and zero mass) is approached. The increase is due to the transmission of ions down the field structure in the absence of an analyzing electric field. As suggested in the previous report, the height of the peak may be a measure of total ambient density, thus eliminating the need for an additional gauge.

Tests performed during the quarter yielded no consistent relation between the height of this peak and the density of the gas as determined from an ionization gauge. This was attributed chiefly to ionizing electrons which, under some conditions of operation, had sufficient energy to reach the collector and partially neutralize the positive ion current. Operation of the filament at a potential positive to the collector did not completely remove the inconsistencies. Residual magnetic fields and, at the higher pressures, scattering of the ion beam by collisions could also destroy the desired linear relationship.

Each of the effects could be eliminated or reduced to negligible proportions by the application of a small rf voltage to the rods. In this manner, heavy particles are focused down the field and electrons are removed. This type of operation is equivalent to working along the q-axis (a = 0) in the stability diagram (Fig. 4 of the previous report). All values of q below 0.91 are stable. Since

$$q = \frac{4eV}{mR_o^2 \omega^2} \qquad (1)$$

all ions are stable at low values of V ($q < 0.91$). As V is increased, ions will become unstable in order of increasing mass and be successively removed from the beam. Figure 1 compares operation in this mode with the conventional spectrum obtained for the same gas mixture. The resolution of the conventional spectrum is low because the ratio of U/V_{rms} was set at only 0.22 to insure 100% transmission. Hence no identification of the peaks will be made beyond indicating that the center peak is due to nitrogen and a small peak near the far left is due to helium. The flat portion of both traces at two major divisions at the far left is due to failure of the rf supply to operate at low applied voltages and is not characteristic of massenfilter operation.

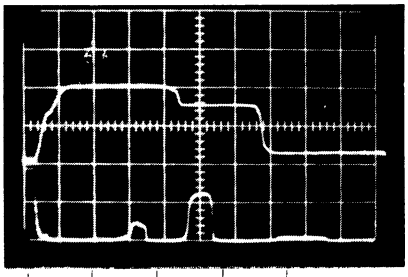

Staircase Sweep —— $U/V_{rms} = 0$
Normal Sweep —— $U/V_{rms} = 0.22$
$R_o = 0.206$ in. $f = 2.39$ Mc
$D_{in} = 0.043$ in. $\theta = 5.1°$
$P = 2.24 \times 10^{-5}$ mm Hg. $I_e = 2.8$ ma
Vertical Scale: 2×10^{-10} amp/cm
$V_e = 67\text{-}1/2$ volts $V_I = 45$ volts

Fig. 1. Massenfilter spectra; normal and "staircase."

The following observations can be made from Fig. 1.

i. With a = 0, a peak is reached and maintained for a large range of amu.
ii. Thereafter, the ion current drops off in a series of steps so that the trace resembles an irregular staircase.
iii. Correlation of the step heights with the corresponding peaks yields exactly the same amplitudes within the limits of observational accuracy.
iv. The stability diagram (previous report) indicates that the step should occur at 1.29 V_{rms} where V_{rms} is the voltage at which the conventional peak is obtained with maximum resolution. This ratio has been verified.
v. The peak level of the first step is not reached until a voltage corresponding to about 8 amu is applied. This is due to the gradual recession from the stability limits at low values of q. As a result, the small helium peak in the conventional trace appears as a perturbation on the rising portion of the "staircase" at low values of V_{rms}.
vi. The staircase has not reached zero at the maximum excursion (approximately 55 amu).

The last observation led to a determination of the source of remaining ion current. Since a mercury diffusion pump was used, the mercury ion (amu = 201) was immediately suspected. To extend the upper limit of the mass range to above 300 amu, the operating frequency was reduced from 2.39 to 1.00 Mc. By Eq. (4.2.9) of the previous report, the attainable resolution is expected to decrease by a factor of 5 or more, all other conditions remaining the same.

Figure 2 is typical of the results obtained at the reduced frequency. The residual ion current is shown to be due to singly ionized mercury with minor contributions by doubly and triply ionized mercury. The three spectra of Fig. 2, taken at successively higher pressures, indicate that the effects of mercury are suppressed with increasing pressure as might be expected.

The following conclusions are based on the above series of tests and observations.

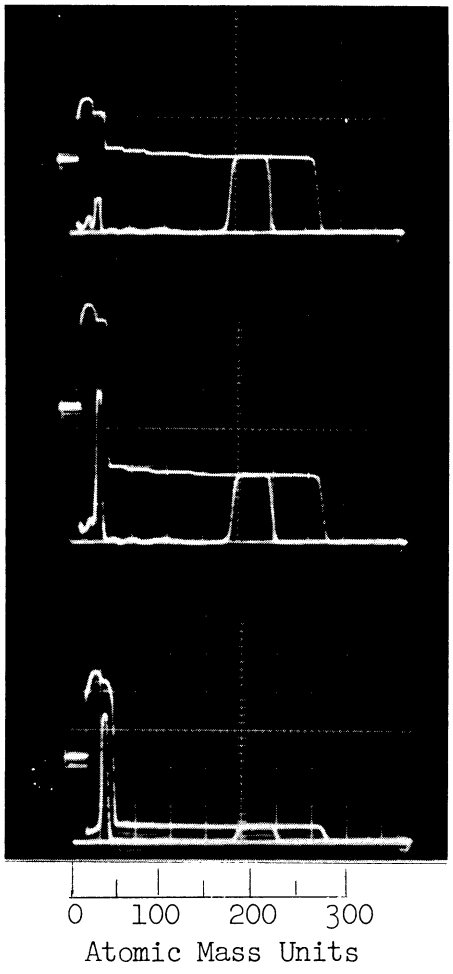

$P = 1.2 \times 10^{-5}$ mm Hg.
Scale: $.5 \times 10^{-10}$ A/cm.

$P = 4.9 \times 10^{-5}$ mm Hg.
Scale: $.5 \times 10^{-10}$ A/cm.

$P = 2.6 \times 10^{-4}$ mm Hg.
Scale: 2×10^{-10} A/cm.

Staircase Sweep -

$U/V_{rms} = 0$

Normal Sweep -

$U/V_{rms} = .20$

$R_o = 0.206"$

$f = 1.0$ Mc.

$D_{in} = 0.031"$

$\theta = 5.2^{o}$

$I_e = 2$ ma.

$V_I = V_e = 45$ Volts

Fig. 2. Massenfilter spectra; low-frequency, large mass range.

i. With the exception of gases lighter than 8 amu, the massenfilter can be calibrated to operate at a = 0 to indicate total density. The limitation at low amu is not considered significant to the purposes of the research

ii. The zero d-c voltage sweep (a = 0) is in itself a good indication of the relative abundances of the major constituents. The rarer species, however, would be difficult to detect in the large amplitudes of the staircase.

iii. The total abundance of those gases having amu's above the maximum excursion of the sweep can be indicated by this method. While no ambient gas above about mass 46 is seriously expected, this feature does raise the possibility of detecting and compensating for leaks from the instrumentation cannister itself if the pressurizing gas is rich in a heavy constituent such as krypton or xenon.

iv. Based on the foregoing, in-flight operation of the massenfilter at 0 volt direct current once out of each 12 sweeps is definitely planned. In addition to providing total density information and data on gases beyond the range of mass sweep, it provides a valuable backup to the normal spectra in the event of rectifier failure leading to U/V_{rms} ratios beyond cutoff.

3.2. MASS CALIBRATION

Previous tests have resulted in massenfilter spectra in which the observed positions of the peaks did not agree with the theoretically determined mass scale given by

$$V = 7.22\ Af^2R_o^2 \text{ volts peak} \quad . \qquad (2)$$

Errors were typically 10%-15% which made positive identification of any but the major peaks impossible. During the quarter, a careful check of the voltage-mass relation was made. The resulting spectra are shown in Fig. 3. Here, the ratio of U/V_{rms} has been increased to a value close to cutoff to increase resolution at the expense of 100% transmission. The gas is the residual left in the system and that due to a small leak. The major N_2 peak is off scale to make observation of the minor peaks possible. From top to bottom, the energy of the ionizing electrons was 90, 67.5, and 45 volts, respectively. In conjunction with the spectra of Fig. 3, the a-c rod voltage, V, was measured at the apex of most of the peaks. Substituting the values of f and R_o in Eq. (2), N_2^+ should appear at 224 volts rms. The measured value was 222 volts. Tabulated on the following page are the measured voltages for most of the peaks of Fig. 3, starting from the left. Also tabulated are the calculated masses (based on N_2^+ equivalent to 222 V_{rms}), the assigned amu (to the nearest integral number), and the identification of the ion.

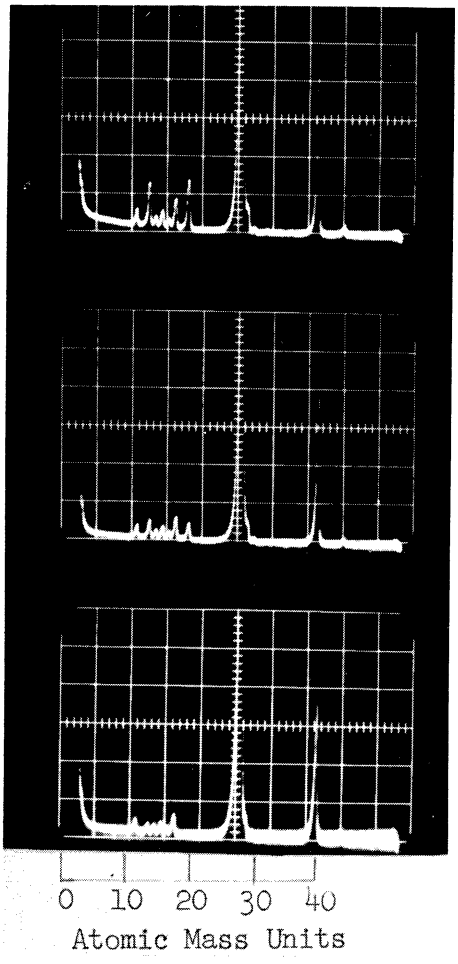

V_e = 90 Volts
P = 4.4 x 10^{-5}mm Hg.
Scale: 0.2 x 10^{-10}A/cm.

V_e = 67.5 Volts
P = 4.4 x 10^{-5}mm Hg.
Scale: 0.2 x 10^{-10}A/cm.

V_e = 45 Volts
P = 4.3 x 10^{-5}mm Hg.
Scale: 0.1 x 10^{-10}A/cm.

Normal sweep - High Resolution

U/V_{rms} = 23.8

R_o = 0.206"

f = 2.39 Mc.

D_{in} = 0.031"

θ = 5.2°

V_I = 45 Volts

Fig. 3. High-resolution massenfilter spectra.

MASS SPECTRA IDENTIFICATION

Peak No.	V_{rms}	amu (Calculated)	amu (Assigned)	Identity
1	94	11.83	12	C^+
2	111	14.0	14	N^+
3	118	14.9	15	CH_3^+
4	127	16.0	16	CH_4^+
5	133	16.8	17	OH^+
6	142	17.9	18	H_2O^+
7	158	19.9	20	A^{++}
8	222	(28)	(28)	N_2^+
9*	---	----	29	$N^{14}N^{15+}$
10*	---	----	30	NO^+
11	---	----	32	O_2^+
12	317	40	40	A^+
13	347	43.8	44	CO_2^+

*Identification tentative.

The peaks at 14 and 20 are determined to be due to N^+ and A^{++} because of the rapid increase of their relative intensity with ionization potential. The peaks at 30 and 32 are barely perceptible and might be overlooked as noise except that a small perturbation in the base line is consistently noted at these points.

4. ION SOURCE

4.1. BASIC DESIGN CRITERIA

The previous report indicated the desirability of a more efficient ion source having the following characteristics:

i. Reduced probability of ambient neutral molecules experiencing a collision with a solid surface prior to ionization.
ii. Increased electron current capability.
iii. Increased efficiency of the electron beam, i.e., a greater proportion of electrons useful for ionization.
iv. Utilizing a greater proportion of the created ions for analysis by focusing them on the inlet port.

Characteristics ii through iv are desirable to increase the sensitivity of the device; i, to yield an ion analysis closely indicative of the ambient neutral composition. The latter is to be accomplished by forming the ions in a volume from which the total solid angle subtended by solid material is held at the minimum possible value. This implies formation of ions at a distance from the inlet port (4 in. has been the dimension selected) and in a volume formed by grid structure. Figure 4 is a photograph of a test model which illustrates the type of construction in progress. Electrons are obtained from three hairpin filaments (F) operated in parallel. The electrons are then accelerated toward the ionizing volume by the grid (G). Ions created in the volume are accelerated toward the first cylinder (L_1) of the lens system by virtue of the field gradient established by the grid (G) and the grid structure at the end of L_1. Focusing of the ions on the inlet port (P) occurs because of the potential difference between L_1 and the second cylinder (L_2). Emerging from the inlet port, the ions enter the rod structure of the four-pole field where mass separation is accomplished. The planar structure of the ionizing volume shown in Fig. 4 has been selected to produce a parallel ion stream to improve the focusing property of the lens system.

4.2. LENS SYSTEM

Several solid models of the cylindrical lens system were constructed and tested, the earliest of which was illustrated in Fig. 18 of the previous report. The final test model, shown in cross section in Fig. 5 and pictorially in Fig. 6, was constructed of steel blocks to achieve accurate alignment. Tests were conducted using the circuit of Fig. 7. Orthogonal sets of deflection plates were included to compensate for any residual misalignment. Data were taken at deflection voltages which yielded peak ion current. Due, in part, to the short lever arm of the beam beyond the deflection plates, peaking in this manner is

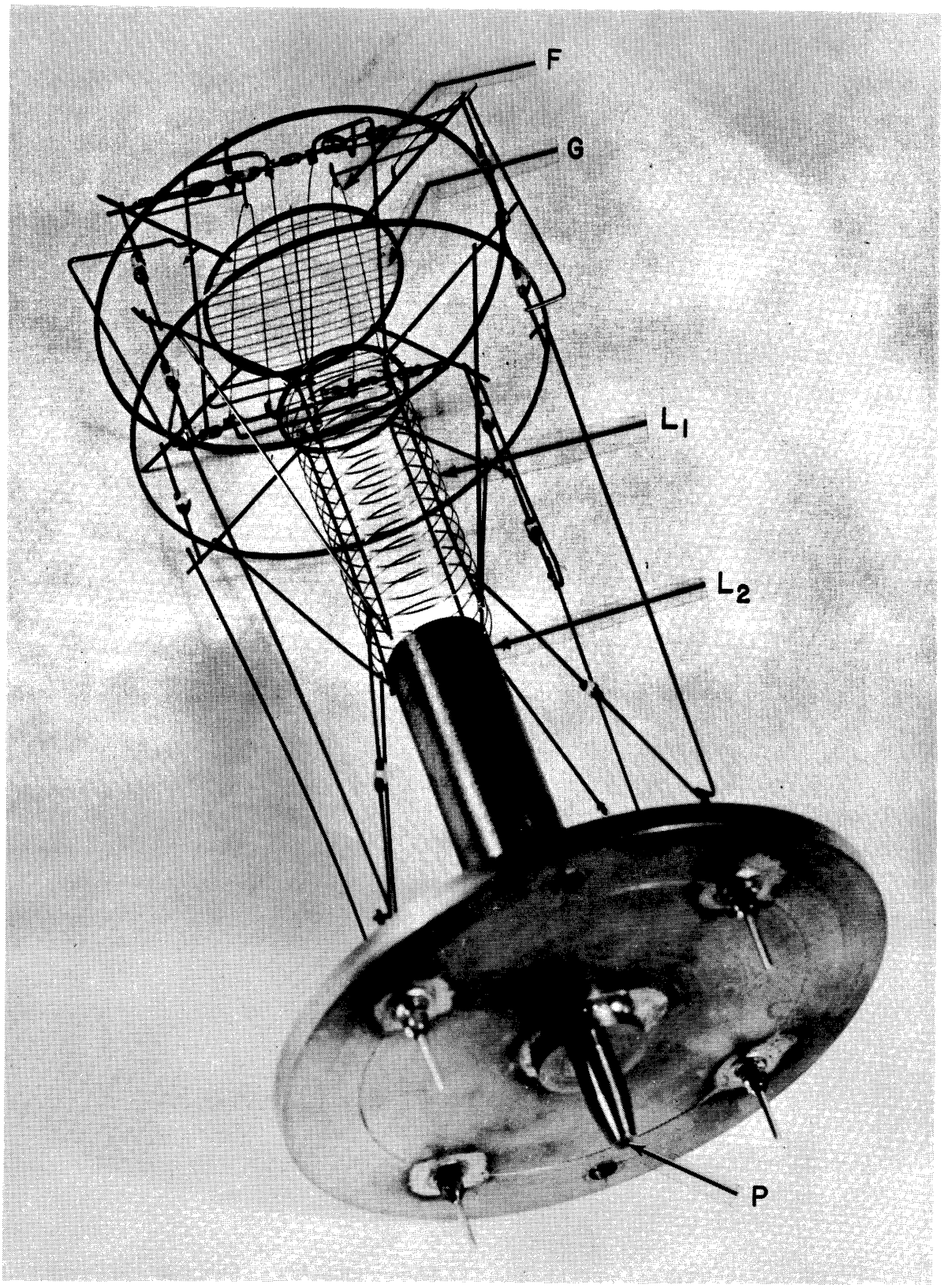

Fig. 4. Ion-source construction.

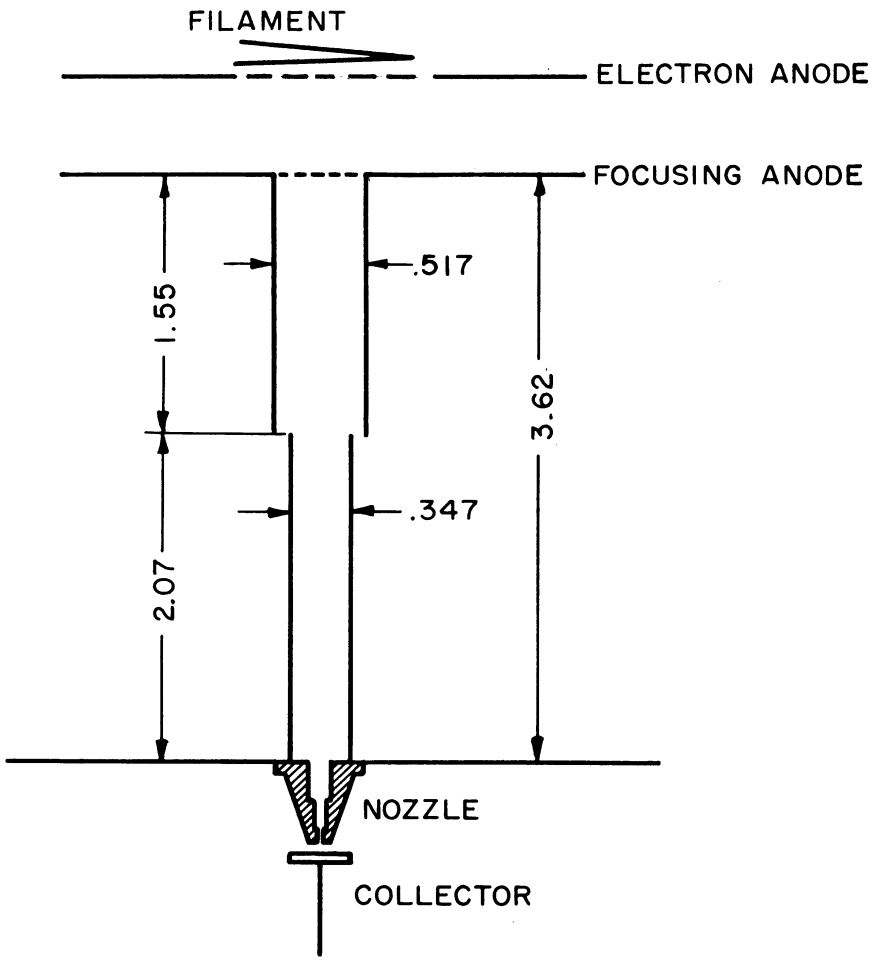

Fig. 5. Ion-source cross section.

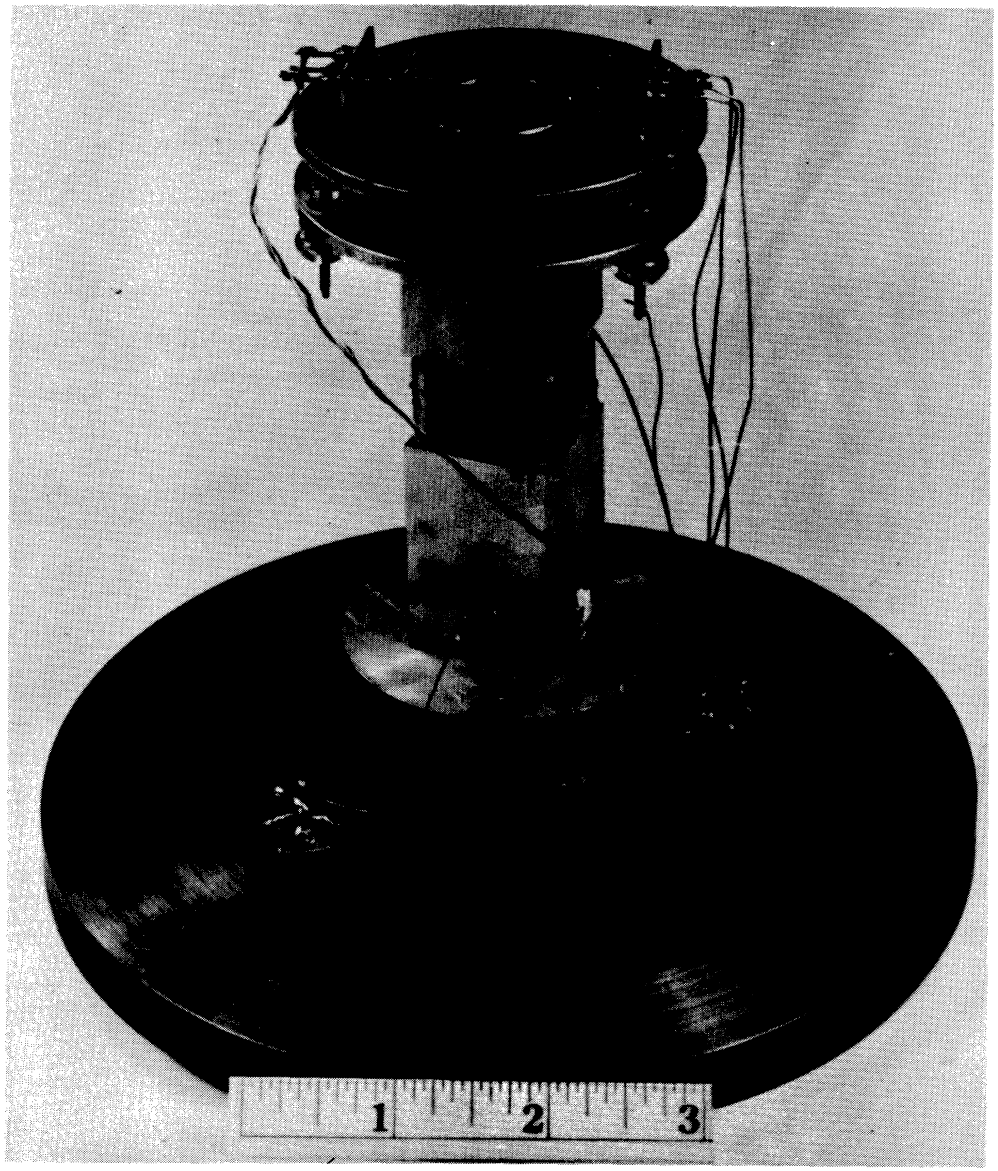

Fig. 6. Ion-source test model.

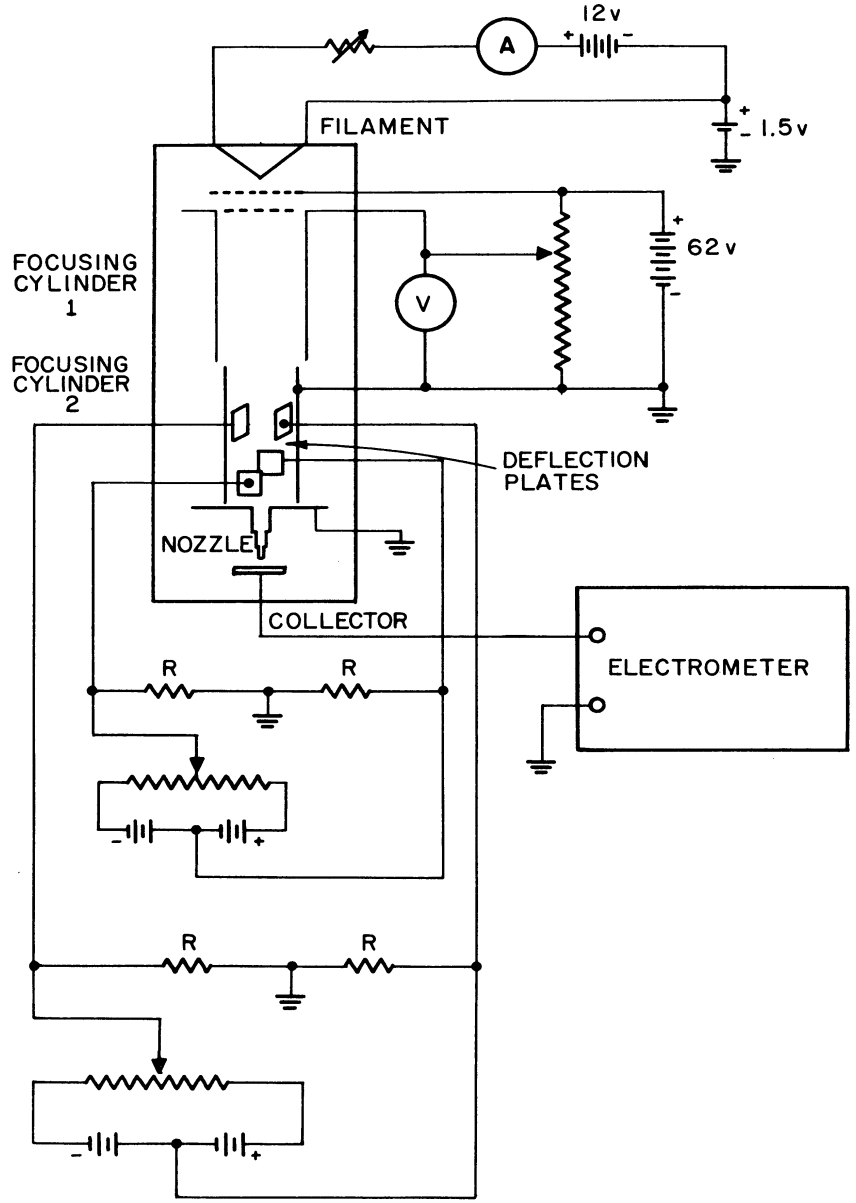

Fig. 7. Ion-source test circuit.

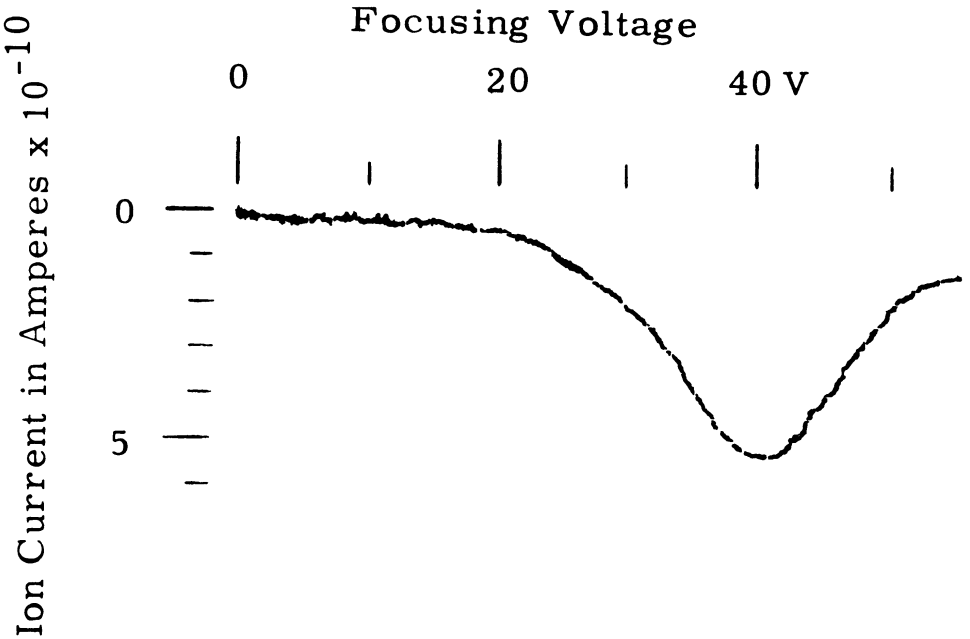

Fig. 8. Ion current as a function of focusing voltage.

quite broad. Maximum ion-current values were obtained with only a few volts on the deflection plates and were less than 10% greater than those obtained with no deflection voltages.

Figure 8 is a plot of ion current vs. focusing voltage. It will be observed that peak ion current occurred at about 41 volts with a total ion-accelerating potential of 62 volts. Based on the dimensions of the lens system (Fig. 5), the theoretical focusing voltage is 46.5 volts. The difference is attributable to the fact that ions are created throughout the ionizing volume and, in general, experience less than the total potential drop of 62 volts. Also contributing to the discrepancy is the fact that the differential equation of an electron (or ion) path through a field of rotational symmetry is true only for particles near the axis and having velocity vectors within a few degrees of the axial direction. In contrast to the usual electron gun and lens system, no effort has been made to restrict operation to particles fulfilling the above criteria since the inlet port imposes the necessary restrictions. This, and the distribution of ion energies, results in a rather indistinct and broad spot at best focus. Broad focusing is no disadvantage for the purpose under consideration and, on the contrary, will help to compensate for small misalignments in manufacture or use.

The peak current obtained from Fig. 8 is approximately 5×10^{-10} amp obtained with an emission current of 10 ma at 62 volts in a system pressure of 3×10^{-5} mm Hg. This corresponds to 0.17×10^{-10} amp per ma emission at 10^{-5} mm Hg and compares with 0.46×10^{-10} amp obtained with the laboratory model described in the previous report. Two factors are responsible for the decrease in sensitivity. First, the electron accelerating grid seen in Fig. 6 is quite coarse, and only about 25% of the total emission current entered the ionizing volume. Second, the ionic path in the new model between creation and admission to inlet port was 4 in. compared to less than 3/4 in. in the laboratory model. The first factor will obviously be alleviated in flight design by use of a finer grid; the second is the price paid to reduce the probability of recombination prior to ionization.

4.3. ELECTRON SOURCE

A prototype hairpin filament and electron accelerating grid assembly was constructed and tested. The model was operated in an atmosphere of oxygen. At 2.3×10^{-5} mm Hg and 6.6 amp of filament current, electron emission was 38 ma at 90 volts. At 1×10^{-4} mm Hg of oxygen and 7.0 amp of filament current, emission was 45 ma. The final flight model, produced with the use of special jigs, is under construction. With the closer spacings made possible by this method, it is expected that the filament will supply as much as 100 ma of electron current at 67.5 volts prior to space-charge limitation.

5. FLIGHT INSTRUMENTATION

A block diagram of the flight instrumentation is given in Fig. 9. This section covers the status of each of the major components with the exception of the massenfilter which is described in Section 3.

5.1. TELEMETRY

All units for the airborne telemetry system are on order and delivery is expected by mid-April.

5.1.1. Antenna.—Excitation of the instrument cannister was considered as a method to radiate rf telemetry signals. The idea was rejected, however, since it would place a voltage maxima at the massenfilter ionization source. A boxed-in slot antenna is impractical because of the unavoidable mechanical interference within the cannister it would introduce. Hence a whip dipole perpendicular to the cannister axis at the back end has been selected. The feed and matching network are actively under development.

5.1.2. Transmitter.—The transmitter selected is the Electro-Mechanical Research (EMR) Model 121-C VHF FM. In this unit, frequency is controlled by a quartz delay line and can be adjusted between 235 and 245 Mc. The units deliver a nominal output of 2.5 watts. One sample unit has been received and delivered 3.1 watts with a supply of 200 volts at 65 ma. Figure 10 shows the transmitter under test.

5.1.3. Subcarrier oscillators.—Four subcarrier channels will be used. Each of three decades of electrometer output will be transmitted via its individual subcarrier channel (Channels 10-12). Channel 9 will be used for monitoring up to twelve points in the circuitry to aid in evaluating the operation of the system. The channels have been selected to yield frequency responses greater than 50 cycles/sec, which will be required to reproduce the signals obtained from the massenfilter and electrometer. EMR Model 184-C subcarrier oscillators have been selected.

5.2. RADIOFREQUENCY OSCILLATOR AND RECTIFIER

Figure 11 is a circuit diagram of the crystal-controlled oscillator and Fig. 12 is a circuit diagram of the high-voltage amplifier and rectifier to drive the massenfilter. The units are shown in Fig. 13 mounted on disks in flight configuration. The oscillator is on the left and the voltage amplifier and rectifier are built on the disk on the right. Minor circuit simplification is underway to eliminate some of the larger adjustable components. In the final flight model, the entire circuit will occupy only one disk.

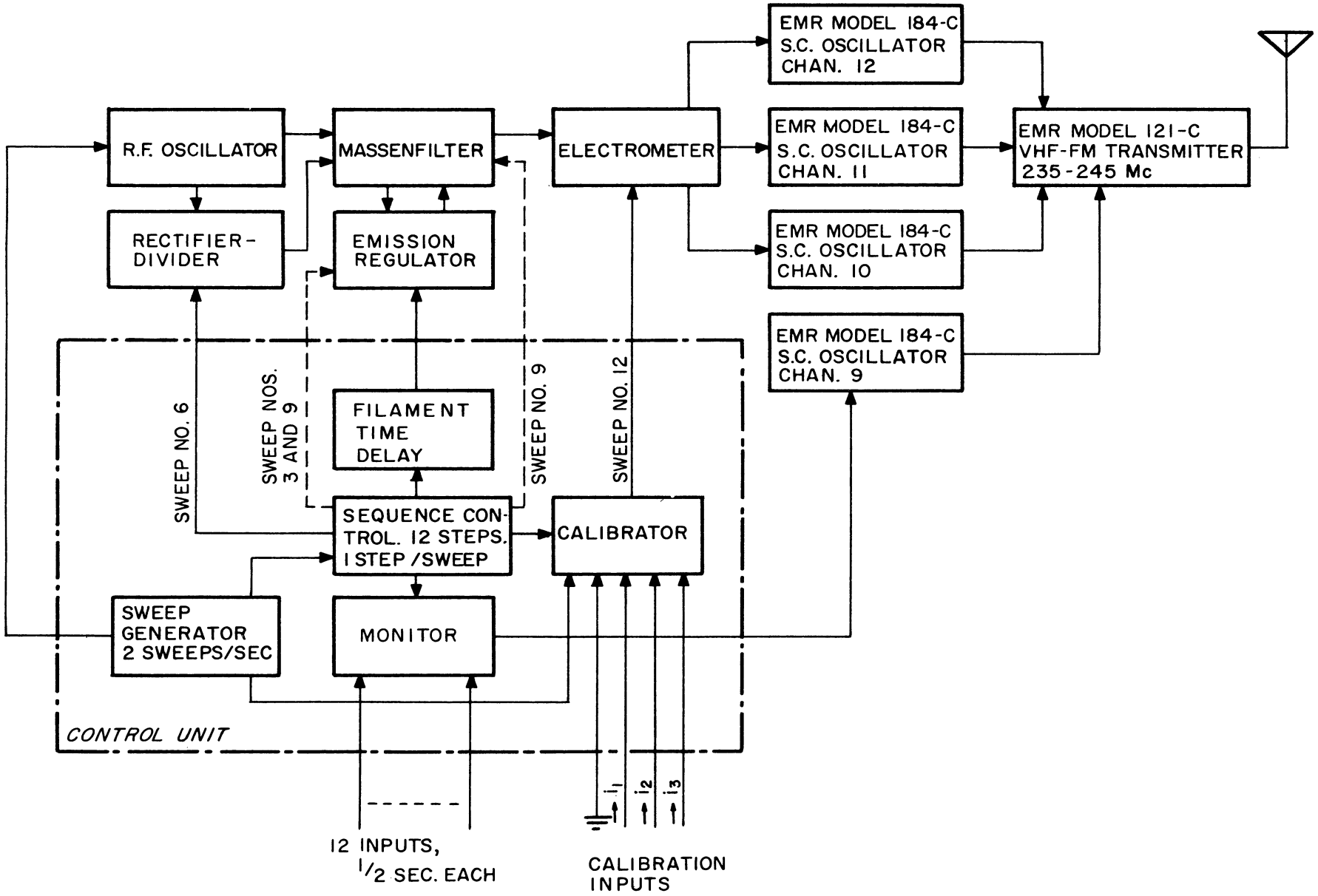

Fig. 9. Flight-instrumentation block diagram.

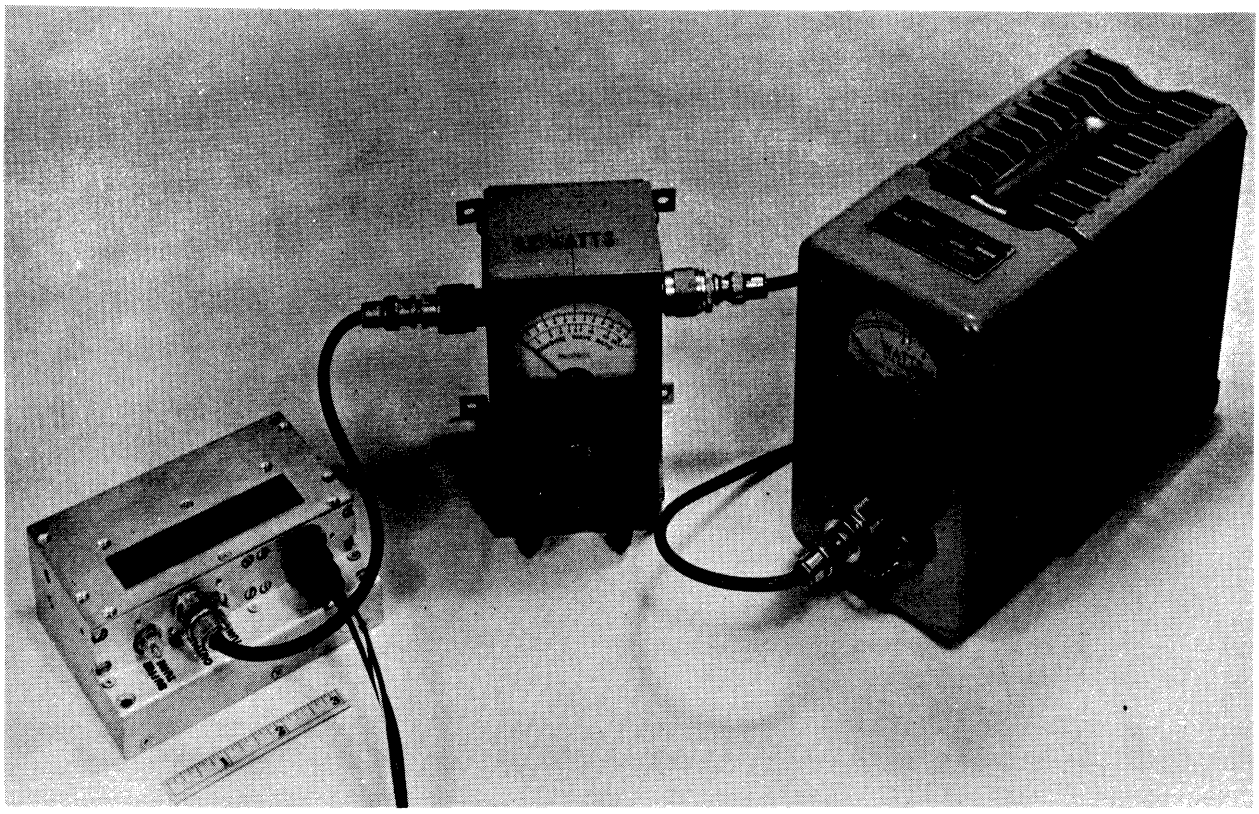

Fig. 10. Flight transmitter under test.

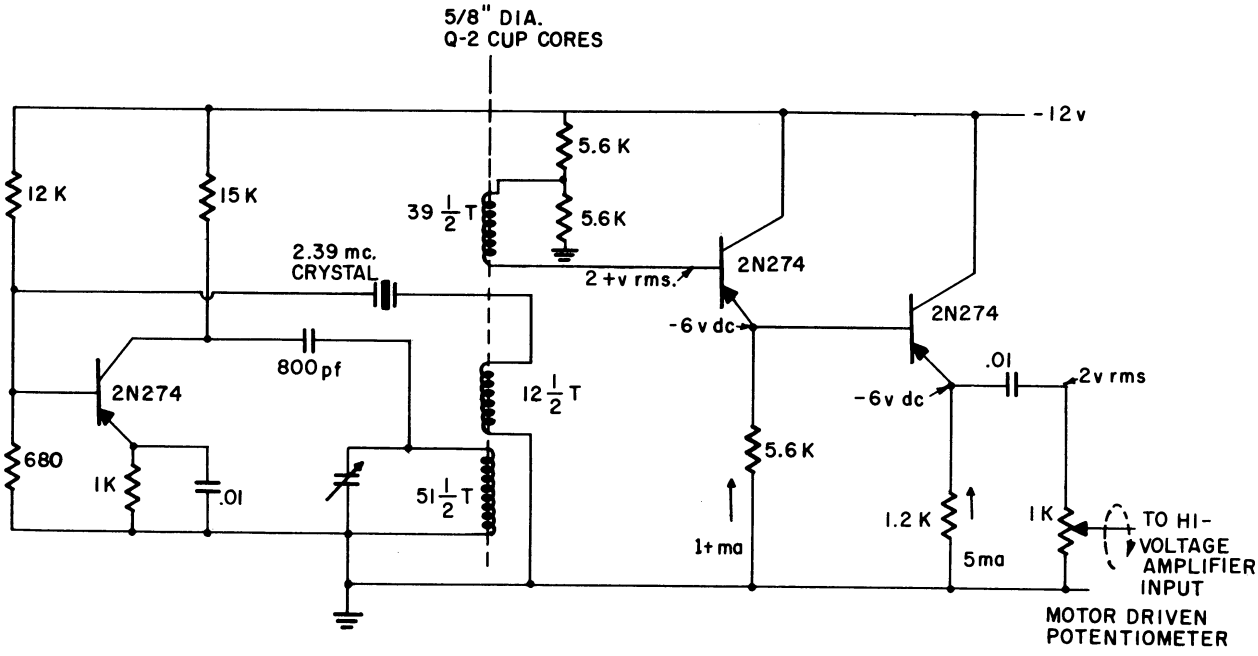

Fig. 11. Crystal-controlled-oscillator circuit diagram.

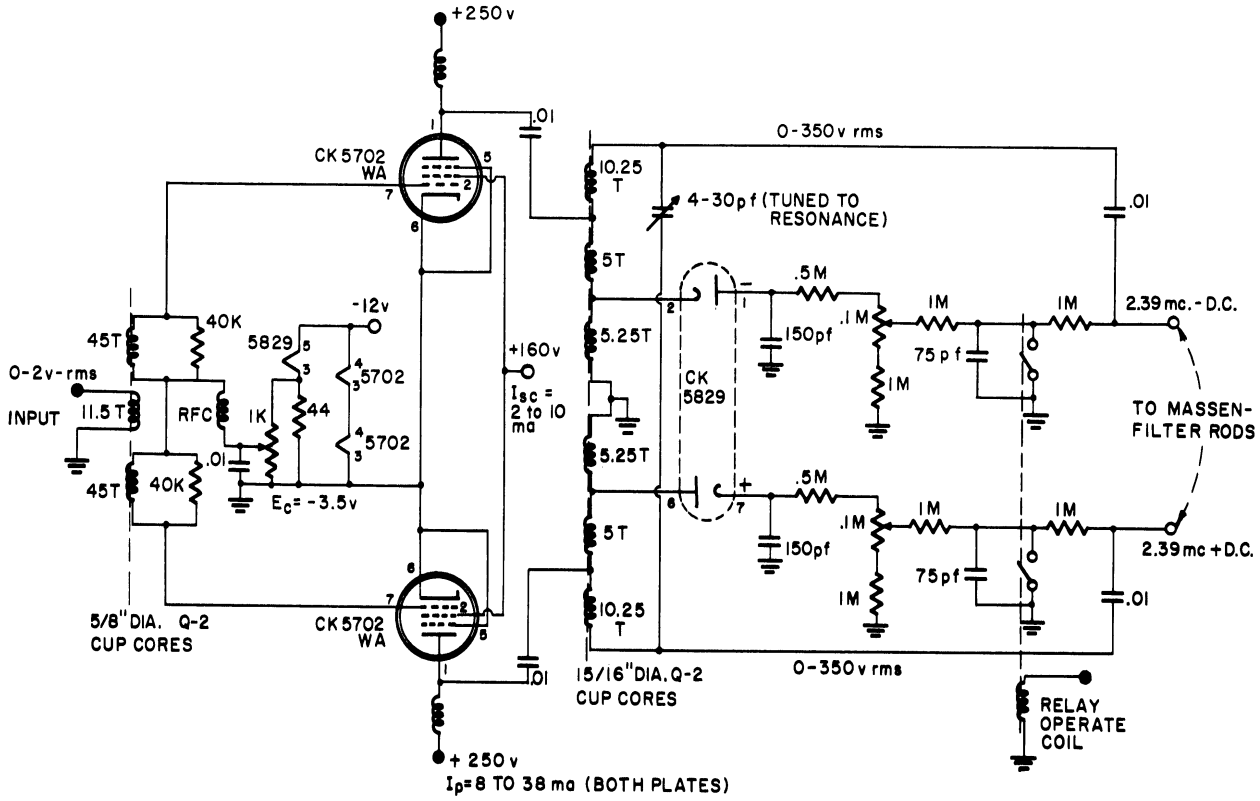

Fig. 12. High-voltage rf amplifier circuit diagram.

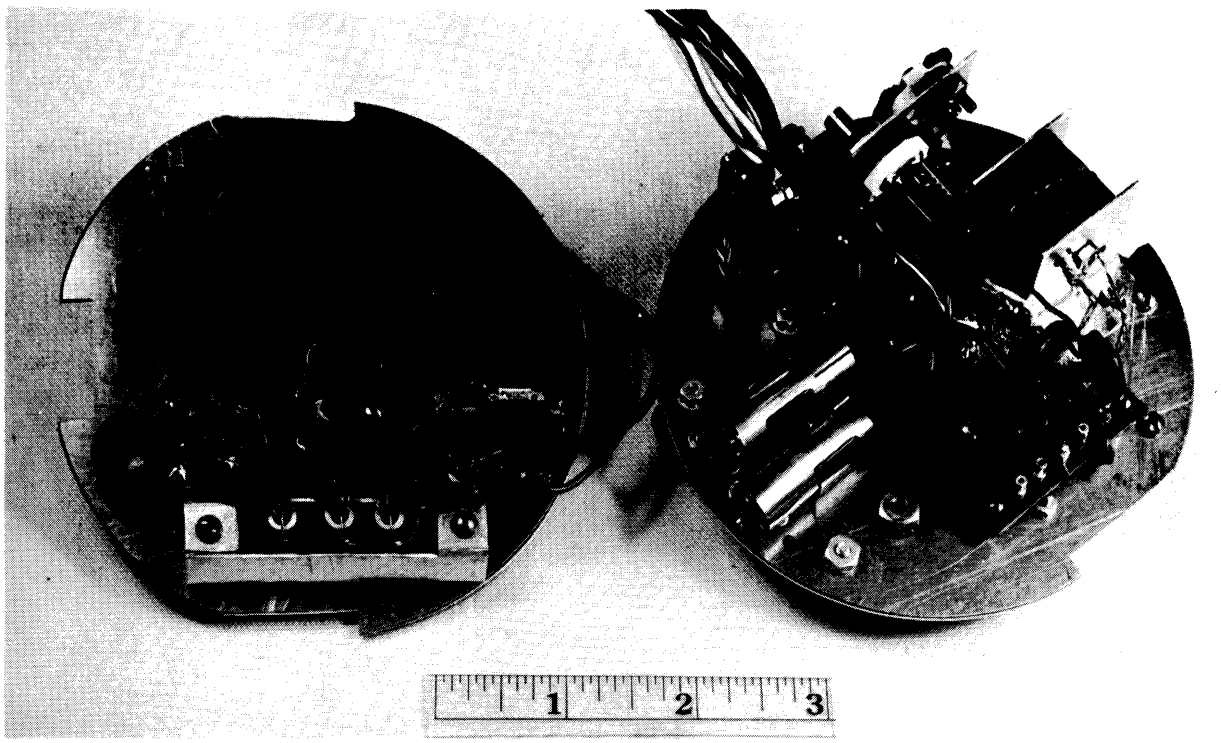

Fig. 13. Flight prototype oscillator and rf amplifier.

An emitter-follower output of the oscillator circuit is used to drive a 1000-ohm potentiometer the shaft of which is motor-driven at 2 rps to produce the sawtooth envelope of the rf voltage required to drive the high-voltage amplifier.

The amplifier-rectifier circuit is standard and self-explanatory. It will be noted the circuit includes a relay which, on closure, shorts the d-c output, thereby removing d-c from the rods to yield the "staircase" spectrum described in Section 3.1. Operation of the relay will be controlled by the sweep-generator and sequence control unit.

Output and linearity are adequate but marginal through amu 44. Along with the minor circuit simplifications in progress, a special effort is being made to extend the upper limit of amu to 50.

A breadboard model of the entire circuitry, using flight components, has been used to drive the massenfilter in analysis of a gas sample containing components with amu up to argon. A motor-driven sweep was used and the repetition rate was varied from less than one to two sweeps per second. No noticeable change in transmission or resolution was observed in the spectra.

5.3. EMISSION REGULATOR

The previous report described a d-c emission regulator circuit which was suitable for flight use. Operation was inefficient, however, because the control transistors regulate by acting as controllable, variable resistors, thereby dissipating the power in excess of that required by the massenfilter filament. Perhaps of greater concern than efficiency is the heating of the transistors and the heat sink which must be provided.

To circumvent these deficiencies, the circuit of Fig. 14 was developed and tested with the laboratory massenfilter as indicated. Here the transistor operates as a switch and regulation is accomplished by maintaining a constant switching rate and varying the on-off duty cycle as required for constant electron emission. Since the transistor is either full-on or cutoff, heat generation is at a minimum.

The 1-kc square wave driving input (obtained from one of the power supplies) is differentiated at the input of transistor Q_1 which amplifies and rectifies the resultant pulses so that its output is a series of positive pulses occurring at the rate of 1000 per second. Transistors Q_2 and Q_3 comprise a one-shot multivibrator. Each positive pulse puts Q_2 in conduction and Q_3 is turned off by the negative voltage step at the collector of Q_2 coupled to the base input of Q_3. Transistor Q_3 is maintained in cutoff while the coupling condenser charges through the 3000-ohm bias resistance in series with the collector circuit of Q_2. At the instant the base voltage of Q_3 reaches a value equal to that on its emitter, Q_3 begins to conduct. Due to the common emitter resistance and the coupling from

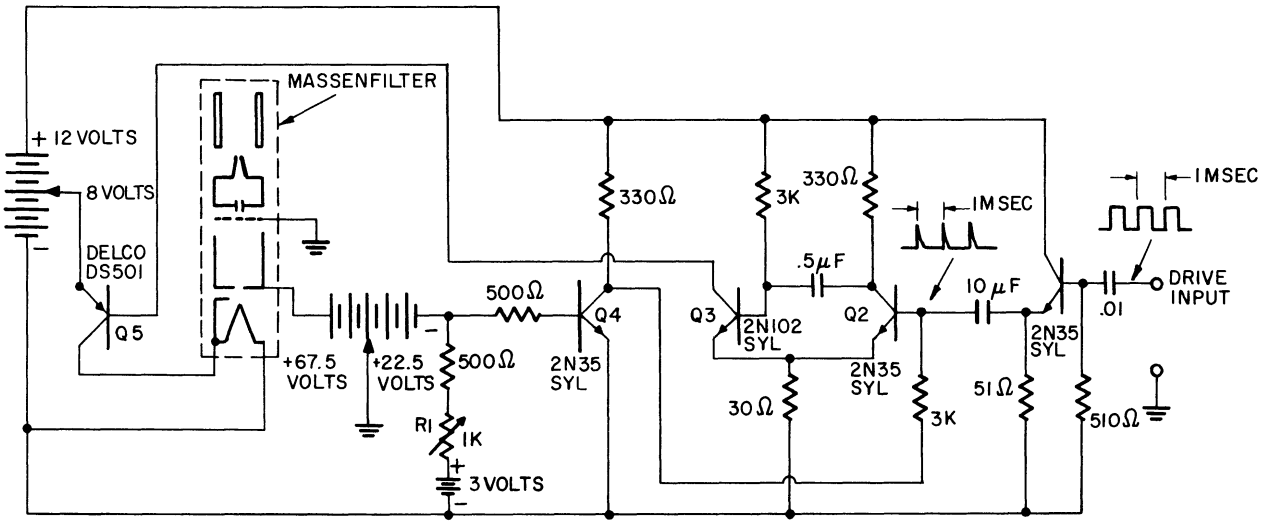

Fig. 14. Duty-cycle emission-regulator circuit diagram.

collector of Q_2 to base of Q_3, the process avalanches so that Q_3 goes quickly into full conduction where, because of the forward bias on its base, it remains until the next driving pulse occurs on the base of Q_2. While Q_3 is in conduction, the coupling condenser discharges through the 330-ohm collector resistance of Q_2 in series with the base circuit of Q_3 with a much shorter time constant than in the reverse mode. Though shorter, this time constant imposes a limit on the minimum time Q_3 must remain in conduction. In the present circuit, the lower limit is approximately 35% of the duty cycle with a driving frequency of 1 kc. Conversely, the circuit will operate up to a point where Q_3 is in conduction essentially all of the duty cycle. Since the control transistor, Q_5, is in conduction simultaneously with Q_3, the fraction of time the massenfilter filament is turned on can be varied through a range of nearly 3 to 1 with the circuit. Because the resistance of the filament increases with the fraction of "on" time, the range of power input is less than 3 to 1. The actual range of filament power will depend on the final filament design and remains to be determined.

The length of time Q_3 is cutoff following a positive pulse on the base of Q_2 is determined by the magnitude of the negative step at the collector of Q_2 which, in turn, is determined by the forward bias on its base. When there is no electron emission in the massenfilter, the voltage at the base of Q_4 is essentially the reference battery voltage and Q_4 is in full conduction. As a result, the forward bias at the base of Q_2 is low, the voltage step at its collector following a driving pulse is small, and Q_3 quickly returns to conduction. Under these conditions, the filament is on almost 100% of the time and heats up rapidly. As emission current increases, the base of Q_4 approaches the emitter voltage and Q_4 begins to cutoff, increasing the forward bias at the base of Q_2 and hence, the time interval the filament is cutoff. Regulation occurs near the value of emission current at which the voltage drop in the series resistances

balances the reference battery voltage. The current value can be adjusted by means of the series resistance.

At regulation, the electron accelerating voltage is essentially equal to the battery voltage (67.5 volts in Fig. 14). The ion-accelerating voltage can be adjusted by the position of the ground tap on the battery and is set at 45 volts in the circuit of Fig. 14.

The circuit has been tested with the laboratory massenfilter and the spectra so obtained were compared with those obtained in the usual d-c operation. With the exception of 1-kc ripple at the peaks of ion current, no difference was discernible. The flight electrometer frequency response will be adjusted to cutoff beyond 50 cps so that the 1-kc ripple components will be rejected.

Figure 14 does not necessarily represent the flight circuit since the values must be tailored to the final flight filament and the pre-established value of emission current. These adjustments can be easily made, however, as soon as a flight model filament is available for test.

5.4. CONTROL SECTION

As indicated in Fig. 9, the sweep generator, sequence control, filament time delay, monitor, and calibrator are all contained in one unit.

5.4.1. Sweep generator. Since the sweep rate and timing functions are not particularly critical, the sweep generator will consist of a simple governor-controlled d-c motor geared down to 2 rps. The motor shaft will drive the sweeping potentiometer discussed in Section 5.2. In addition, the motor shaft will drive a wafer switch which will connect to four calibration inputs in turn, completing a cycle with each revolution of the shaft. Finally, the motor shaft will drive the sequence control unit.

5.4.2. Sequence control and calibrator. The sequence control consists of a wafer switch driven by the motor shaft through an intermittent planetary gear system such as used in counters. These gears have the property of indexing an output shaft one step for each revolution of the input shaft. Between indexing periods, the output shaft is locked. The gear systems are commonly supplied in decade units yielding steps of 36°. Satisfactory gears are immediately available and will be used, if necessary. Steps of 30° with 12 positions are preferable, however, and attempts to obtain satisfactory gears of the latter type are underway. The sequence control will remove the d-c rod voltage to obtain a "staircase" spectrum (Section 3.1) on sweep No. 6. The calibrator output will be impressed on the electrometer input during sweep No. 12 during which three reference currents and zero will be sent through the electrometer circuit. Also under consideration is the search for ambient ions by turning off the filament. The dotted lines in Fig. 9 indicate this function. Two sweeps, Nos. 3 and 9, may be devoted to the ambient ion composition, one for positive and one for neg-

ative ions. The remainder of the sweeps will be normal to yield ambient gas composition spectra.

5.4.3. Monitor. The monitor is simply a wafer switch driven by the sequence control output shaft. Thus up to 12 different circuit points can be monitored sequentially, 1/2 second devoted to each point.

5.4.4. Filament time delay. This unit consists of a wafer switch driven by another set of intermittent planetary gears, similar to and driven by the first. The unit will complete a cycle in 72 seconds and, for protection, will be used to delay turning on the filament until a predetermined time after ejection of the instrument cannister. Preliminary study indicates a delay greater than 6 seconds is desirable; hence, the additional stage. Depending on success in obtaining 12-step gear systems, the sequence unit may also be used to control the time of cannister ejection after missile launch. As a backup, however, three Haydon timers having a 90-second cycle are on order to perform this function. The timers, if used, will be located in the compartment below the instrumentation cannister.

5.5. ELECTROMETER

The electrometer is the major item of Fig. 9 which remains to be completed. An initial design has been made and tests have begun.

The electrometer will consist of three sections, each comprised of an operational amplifier with total feedback. The input section will be a vacuum tube balanced amplifier, designed for minimum drift and input current. A 50-megohm feedback resistor will give a full-scale sensitivity of 1×10^{-7} amp.

For the remaining two sections, one with a gain of 10 and the other with a gain of 100, a study of transistor circuits has been made to determine their applicability. Since these are driven by the first section with a relatively low output impedance, input current specifications can be relaxed but not ignored. Of particular interest is a circuit described in the literature using a boot-strapped emitter-follower input. Easily obtainable input impedances of 100 megohms are claimed. This type of circuit is under investigation.

5.6. POWER SUPPLIES

Primary power will be obtained from Yardney Silvercels because of their high energy to volume and weight ratios and because of their relatively flat discharge characteristics. High-voltage power will be obtained from transistorized d-c—d-c converters. Final design of these awaits completion of the remainder of the circuitry. An initial unit to provide power to the massenfilter oscillator and amplifier has been designed and built. A circuit diagram is given in Fig. 15 while photographs of the unit appear in Figs. 16 and 17. The operation of the circuit is standard and requires no description here.

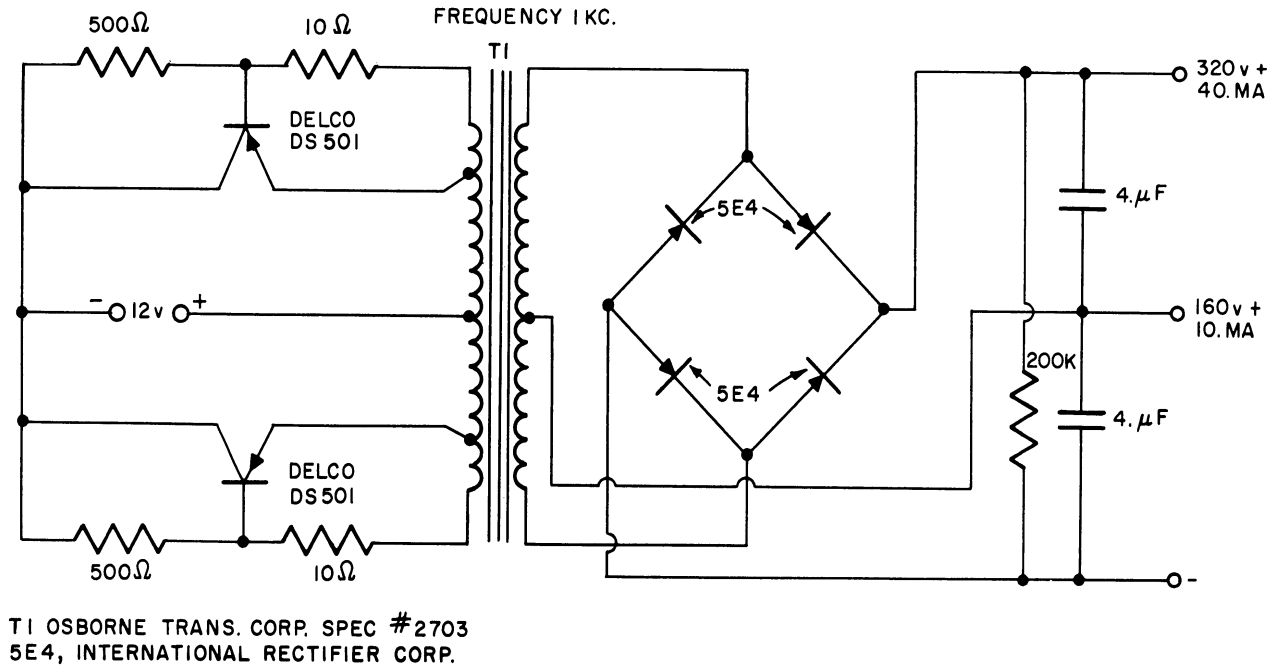

T1 OSBORNE TRANS. CORP. SPEC #2703
5E4, INTERNATIONAL RECTIFIER CORP.

Fig. 15. Transistor-power-supply circuit diagram.

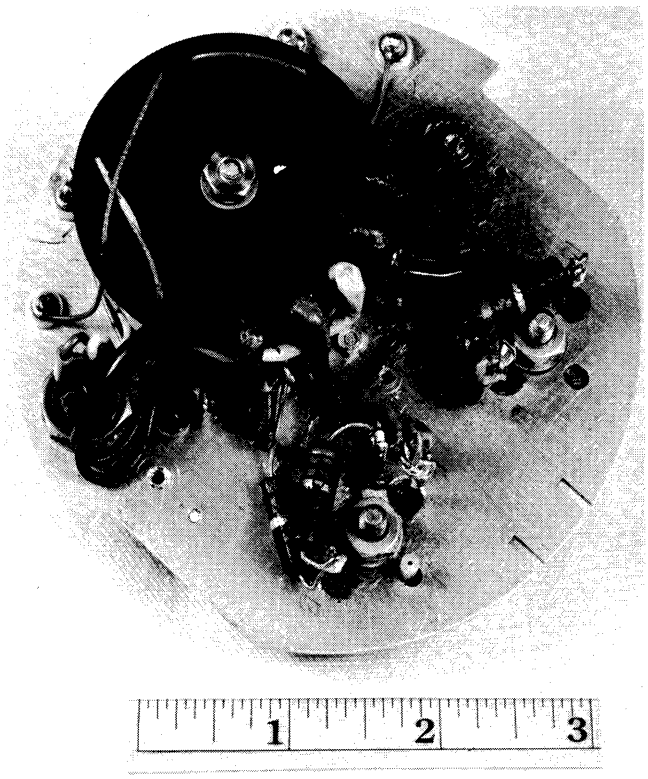

Fig. 16. Transistor power supply; side 1.

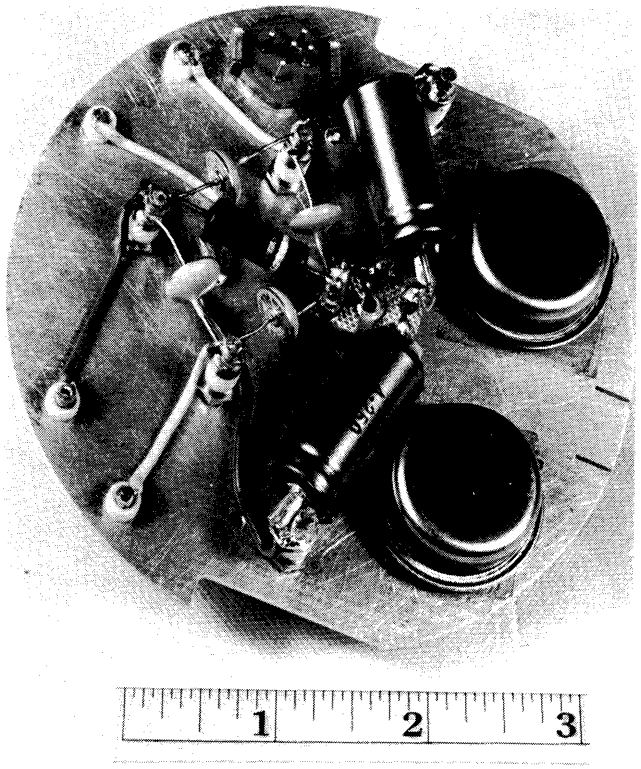

Fig. 17. Transistor power supply; side 2.

6. INSTRUMENTATION PACKAGE

Layout drawings of the instrumentation package have been completed and materials have been received. Detail drawings are about half complete. Fabrication of the parts for the instrumentation package is underway.

7. GROUND STATION

Figure 18 is a block diagram of the ground station. All items noted in the blocks are on order and are expected to arrive by April 15. The Nems-Clarke receiver has already been received, and the Tektronix oscilloscope, doubling as part of our laboratory test equipment has been in service for some time. The checkout of all units will be complete by May 1.

In addition to the equipment shown in Fig. 18, several pieces of test equipment for the ground station have been placed on order.

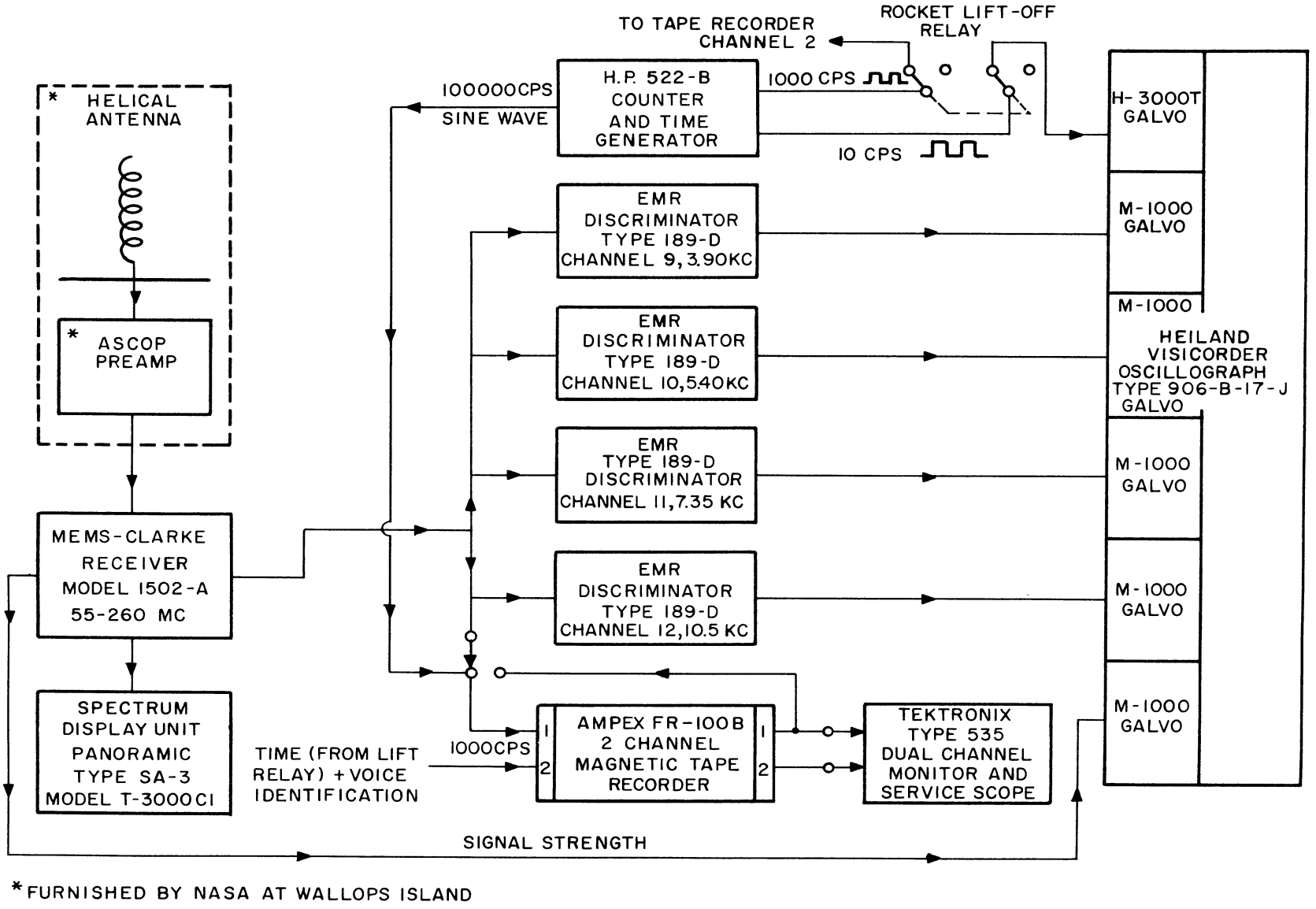

Fig. 18. Ground-station block diagram.

8. VACUUM SYSTEMS

8.1. STAINLESS-STEEL SYSTEM

The system has been placed in operation and pressures of less than 10^{-8} mm Hg are obtained without baking.

8.2. OIL DIFFUSION PUMP SYSTEM

The system has been fitted with an interchangeable glass bell jar for visual observations. It has also been equipped with an adjustable leak to provide rapid and convenient pressure adjustments and is ready for flight massenfilter tests and calibrations.

The procedure to be employed is to balance the full pumping speed of the diffusion pump against the leak rate, thereby providing a constant and controllable pressure in the test chamber. The pumping speed and volume of the system are such that the time constant of the transient between two pressure settings is the order of several seconds. This procedure essentially eliminates the effects of adsorption of gases, particularly oxygen, on the walls of the vacuum chamber and on the apparatus, hot filaments, etc.

9. FUTURE PROGRAM

Final design of all components will be completed and construction of three complete flight units will continue in the next quarter. Firings will be scheduled at Wallops Island six weeks prior to the anticipated dates. As set forth in the previous report, the flights are designed to yield density and composition data from 100 to beyond 200 km. Temperatures and pressures will be derived from reduction of the primary data.

All three units will be scheduled for flight. Firing of the third unit will depend on the degree of success enjoyed in the first two rounds.

The massenfilter orifice configuration for the initial flights has been firmly established. Further tests aimed at optimization with the new ion source will be continued on a noninterference basis.